

Photoluminescent Characterization of Atomic Diffusion in Core-Shell Nanoparticles

J. DiMaio¹, B. Kokuoz¹, T.L. James¹, T. Harkey², D. Monofsky³, and J. Ballato¹

¹Center for Optical Materials Science and Engineering Technologies (COMSET) and the School of Materials Science and Engineering, Clemson University, Clemson, SC 29625
²Clover High School, Clover, SC, ³Carolina Day School, Asheville, NC

Abstract: Eu³⁺ doped LaF₃ nanoparticles with core/shell morphologies were synthesized and selected spectroscopic properties were measured as a function of heat treatment times and temperatures. More specifically, the relative intensity of photoluminescence spectra, both through direct excitation of the lanthanide as well as phonon sideband spectra were evaluated with increasing amounts of time held at specific temperatures. A one dimensional approximation was used to compute an effective diffusion coefficient for the rare earth dopants in LaF₃. Despite the simplicity of the model employed, the calculated diffusion coefficients based on the spectroscopic results are accurate within an order of magnitude in comparison to other fluoride crystals yielding a simplified approach to estimating kinetic and diffusion effects in optical materials.

©2008 Optical Society of America

OCIS codes: (160.4760) Optical properties, (160.2540) Fluorescent and luminescent materials, (160.4236) Nanomaterials, (160.5690) Rare-earth-doped materials, (300.6280) Spectroscopy, fluorescence and luminescence

References and Links

1. J. R. DiMaio, B. Kokuoz, T. L. James, and J. Ballato, "Structural determination of light emitting inorganic nanoparticles with complex core/shell architectures." *Adv Mater* **19**, 3266–3270 (2007).
2. J. R. DiMaio, C. Sabietter, B. Kokuoz, and J. Ballato, "Controlling Energy Transfer between Multiple Dopants within a Single Nanoparticle," *Proc Natl Acad Sci USA* **105**, 1809-1813 (2008).
3. C. F. Hoener, K. A. Allan, A. J. Bard, A. Campion, M. A. Fox, T. E. Mallouk, S. E. Webber, and J. M. White, "Demonstration of a Shell-Core Structure in Layered CdSe-ZnSe Small Particles by X-ray Photoelectron and Auger Spectroscopies," *J. Phys. Chem.* **96**, 3812-3817 (1992).
4. L. E. Brus, "Nucleation and Growth of CdSe on ZnS Quantum Crystallite Seeds, and Vice Versa, in Inverse Micelle Media," *J. Am. Chem. Soc.* **112**, 1327-1332 (1990).
5. A. Häßelbarth, A. Eychmüller, R. Eichberger, M. Giersig, A. Mews, and H. Weller, "Chemistry and Photophysics of Mixed CdS/HgS Collids," *J. Phys. Chem.* **97**, 5333-5340 (1993).
6. M. Darbandi, R. Thomann, and T. Nann, "Single Quantum Dots in Silica Spheres by Microemulsion Synthesis," *Chem. Mater.* **17**, 5720-5725 (2005).
7. K. Kömpe, H. Borchert, J. Storz, A. Lobo, S. Adam, T. Möller, and M. Haase, "Green-Emitting CePO₄ Core-Shell Nanoparticles with 70 % Photoluminescence Quantum Yield," *Angew. Chem. Int. Ed.* **42**, 5513 (2003).
8. O. Lehmann, K. Kömpe, and M. Haase, "Synthesis of Eu³⁺-Doped Core and Core/Shell Nanoparticles and Direct Spectroscopic Identification of Dopant Sites at the Surface and in the Interior of the Particles," *J. Am. Chem. Soc.* **126**, 14935 (2004).
9. J. W. Stouwdam and F. C. J. M. van Veggel, "Improvement in the Luminescence Properties and Processability of LaF₃/Ln and LaPO₄/Ln Nanoparticles by Surface modification," *Langmuir* **20**, 11763-11771 (2004).
10. Z. L. Wang, Z. W. Quan, P. Y. Jia, C. K. Lin, Y. Luo, Y. Chen, J. Fang, W. Zhou, C. J. O'Conner, and J. Lin, "A Facile Synthesis and Photoluminescent Properties of Redispersible CeF₃, CeF₃:Tb³⁺, and CeF₃:Tb³⁺/LaF₃ (Core/Shell) Nanoparticles," *Chem. Mater.* **18**, 2030-2037 (2006).
11. M. J. Dejeneka, "The luminescence and structure of novel transparent oxyfluoride glass-ceramics." *J Non-Cryst Solids* **239**, 149–155 (1998).
12. G. Schneider and G. Decher, "Distance-Dependant Fluorescence Quenching on Gold Nanoparticles Ensheathed with Layer-by-Layer Assembled Polyelectrolytes," *Nano Letters* **6**, 530-5336 (2006).

13. X. Liu, C. Li, Z. Quan, Z. Cheng, and J. Lin, "Tunable Luminescence properties of CaIn₂O₄:Eu³⁺ Phosphors," *J. Phys. Chem. C*, **111**, 16601-16607 (2007).
 14. J. Crank, *The Mathematics of Diffusion* (Oxford University Press, New York, 1975).
 15. D. J. Cherniak, X. Y. Zhang, N. K. Wayne, and E. B. Watson, "Sr, Y and REE diffusion in fluorite," *Chem. Geol.* **181**, 99-111 (2001).
 16. S. Sivakumar, F. C. J. M. van Veggel, and M. Raudesepp, "Bright White Light through Up-Conversion of a Single NIR Source for Sol-Gel-derived Thin Film Made with Ln³⁺-Doped LaF₃ Nanoparticles," *J. Am. Chem. Soc.* **127**, 12464-12465 (2005).
-

1. Introduction

Recent attention has been paid to the use of core-shell structured nanoparticles to yield improved properties and performance. The shell is most often used to provide a chemically-designed environment, to control energy transfer between ions,^{1,2} and to prevent quenching by the external environment (i.e., solvent) as seen in both quantum dots³⁻⁶ and rare earth doped nanoparticles.⁷⁻¹⁰ While these novel structures are of great interest and potential, for practical applications, it is important to know how elevated temperatures and time affect their internal structure and resultant optical properties. One can imagine that with structures on the order of a few unit cells, diffusion can play a significant role in the emission spectra and radiative lifetimes of the nanoparticles.

In this work, photoluminescence and phonon sideband spectroscopies are used to optically determine the severity of diffusion within structured nanoparticles. Europium doped LaF₃ core nanoparticles with varying shell thickness of undoped LaF₃ were used to study these effects.

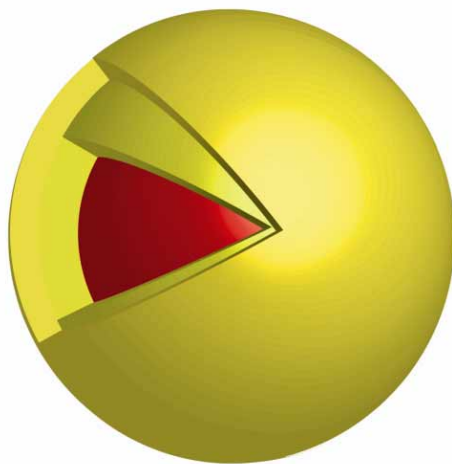


Fig. 1. Model of the europium (red) doped core nanoparticle with a first (middle) and second (outer) layer of undoped lanthanum fluoride (yellow).

2. Experimental

2.1 Nanoparticle synthesis

LaF₃ based core-shell nanoparticles were prepared as described previously.⁹ Briefly, van Veggel, et al., coated active nanoparticles with a passive LaF₃ shell (hereafter called "simple core-shell" structure) in order to minimize quenching by OH vibrations of dopant ions residing on or near the particle surface. In order to synthesize shells of various thicknesses, van Veggel's method for producing simple core-shell structures was extended to produce multiple shells (shown schematically in Figure 1). The current approach employed here for nanoparticle synthesis is as follows: a solution of 614 mg of ammonium di-*n*-octadecyldithiophosphate (ADDP) and 126 mg of NH₄F in 70 mL of ethanol/water was

heated to 75° C. A 2 mL aqueous solution with total molar $\text{Ln}(\text{NO}_3)_3$ concentration of 1.33 mmol was then added drop-wise to the stirring fluoride solution to form the core particles. After stirring for 10 minutes, the first shell was grown by the alternating addition in 10 parts of a 2 mL aqueous NH_4F (126 mg) solution and a 2 mL aqueous $\text{Ln}(\text{NO}_3)_3$ solution with total molar concentration of 1.33 mmol. The composition of the $\text{Ln}(\text{NO}_3)_3$ solution is the composition of the shell. In the majority of this work, 20 weight percent Eu^{3+} was doped into the core of the LaF_3 nanoparticles of 5.5 nm average diameter. For selected experiments, 3 weight percent Eu^{3+} doping was used. After removing a sample of the particles with no shell, an equivalent volume of LaF_3 precursor was added to the solution which allowed the growth of an undoped LaF_3 shell that was ~0.8 nm thick. After removing a sample, another equivalent of undoped LaF_3 precursor was added growing an additional 0.5 nm of shell (1.3 nm total thickness). Thicker shells also were grown and are specifically noted in the discussion section. Particle size analysis was completed by the use of TEM and XRD as discussed in detail elsewhere¹ and the shell growth followed the simple volumetric addition model. All shell thicknesses given in this manuscript are based using those calculations.

2.2 Heat treatment

Eu^{3+} transitions are sensitive to quenching due to dipole-dipole interactions. The $^5\text{D}_3$, $^5\text{D}_2$, and $^5\text{D}_1$ manifolds yield negligible visible emission when concentrations of Eu^{3+} are greater than ~3% or when average the ion-ion distances are greater than ~4 nm.¹¹ In order to determine the effect of diffusion, the samples were annealed at 650 °C in fifteen minute intervals in a tube furnace followed by measuring the photoluminescence. The average distance between Eu^{3+} ions is presumed to increase as the Eu^{3+} ions in the core of the nanoparticle diffuse into the shell, allowing the ions at the leading edge of the concentration gradient to emit from their high energy manifolds; i.e., they are no longer concentration quenched when their overall concentration is now diffused into a larger volume.

2.3 Analytical characterization

Photoluminescence measurements were performed with a Jobin Yvon Fluorolog-3 spectrofluorometer with a double grating configuration with an excitation bandpass of 2 nm and a scan rate of 60 nm/min. All emission scans were performed with an excitation wavelength of 397 nm, while all phonon sideband measurements were made by monitoring the $^5\text{D}_0 \rightarrow ^7\text{F}_1$ (591 nm) emission. TEM was performed on a Hitachi H7600, operating at an acceleration voltage of 200 kV. X-ray diffraction was performed with a Scintag XDS 2000 using $\text{Cu K}\alpha$ radiation. All measurements were made at room temperature,

3. Results and discussion

Changes to the emission spectra as a function of processing time and temperature can be used to understand and quantify both steady state and non-steady state condition for diffusion. Figure 2 shows the emission spectra for the particles as they are heat-treated. It is clear in Fig. 2(a) that there is little change in the emission spectra. Specifically, no increase in the emission intensities from the $^5\text{D}_2$ and $^5\text{D}_1$ manifolds is observed. Instead a decrease in the intensity is observed which is attributed to the surface atoms increased interaction with a phosphorous oxide layer that forms when the dithiophosphate ligands are oxidized during the heat-treatment. In Fig. 2(b), slight increases in the emission is observed and the appearance of the $^5\text{D}_2 \rightarrow ^7\text{F}_3$ occurs, but when a ~1.3 nm shell is added to the core and the particles are annealed, the $^5\text{D}_2$ manifold is much more active in emitting.

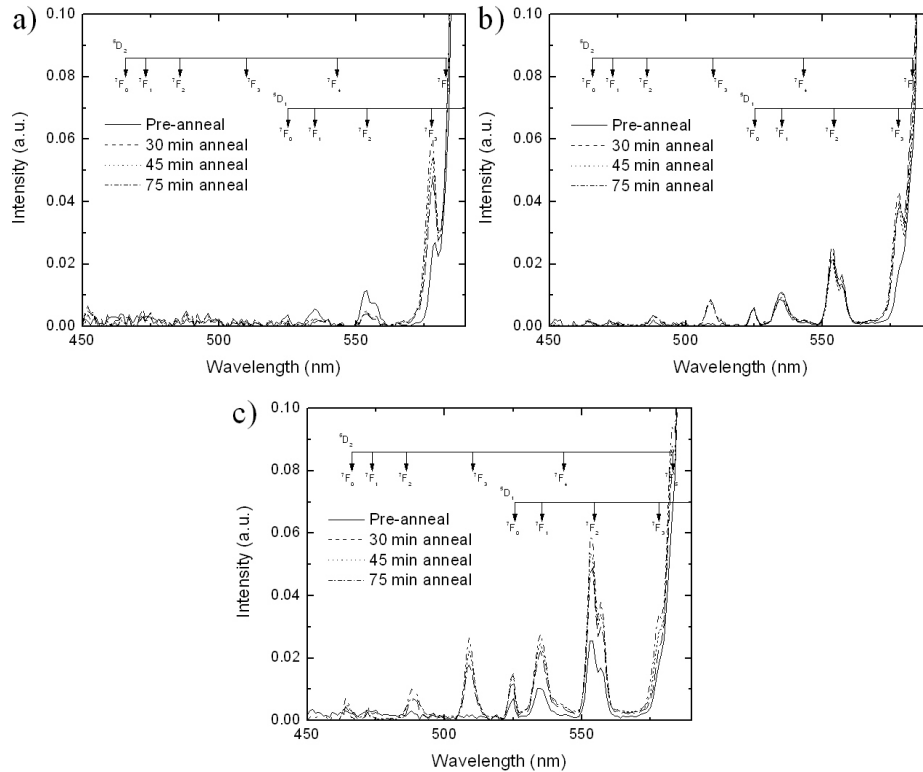


Fig. 2. Photoluminescence of $\text{Eu}_{0.2}\text{La}_{0.8}\text{F}_3$ nanoparticles before and after annealing with (a) no shell and with shells calculated to be (b) 0.8 nm and (c) 1.3 nm thick.

While the photoluminescence provides some information as to the change in the average concentration of the dopant within the particle, phonon sideband spectroscopy can yield complimentary information as to when the Eu^{3+} ions are reaching the surface of the LaF_3 nanoparticles. As the Eu^{3+} ions diffuse from the center of the nanoparticles to the edge, the rare earth ions experience a change in the vibrational environment, as they are now vibrationally influenced by the phosphate group of the ligand. The P-O stretch centered at $\sim 1000\text{ cm}^{-1}$ is clearly visible in particles without shells. Once an intermediate passivating shell was added the phonon sideband peak diminishes. This is seen in Fig. 3. Similar work has been done with the distance-dependent quenching of emission from gold nanoparticles via layer-by-layer techniques.¹²

The phonon sideband (PSB) was also measured (Fig. 4) after each annealing step for the Eu^{3+} -doped particles illustrated in Fig. 1. When the P-O stretch of the ligand begins to appear in the phonon sideband it is assumed that the Eu^{3+} ions have diffused from the core and have begun to reach the surface of the particle. This time can now be used in conjunction with the various shell thickness to determine an effective diffusion coefficient.

It is interesting to note that the intensity of the PSB increases significantly after the first heat-treatment even for the nanoparticles without shells. This is believed due to an increased interaction of the Eu^{3+} ions with the P-O after the sulfur atoms of the ligand were oxidized. In addition, the interaction between the P-O and the Eu^{3+} has most likely strengthened from a weak coordinated bond to a stronger covalent bond. Beyond this, for thicker shells, lower PSB intensities are observed as would be expected. Moreover, it appears that a point of steady state

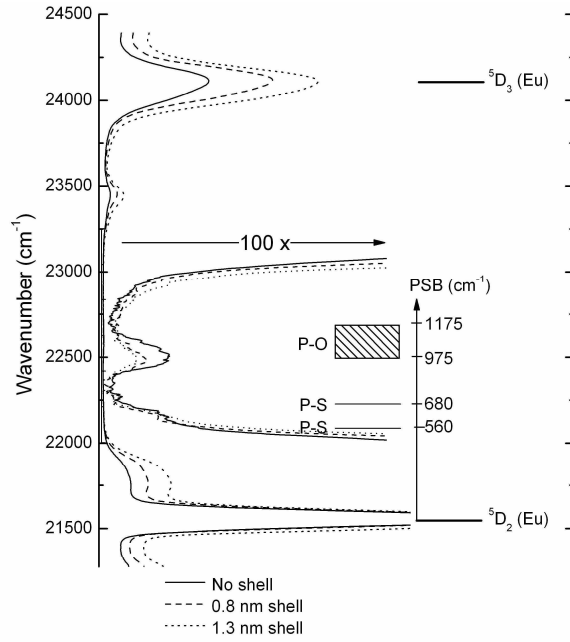


Fig. 3. Phonon sideband spectra of core-shell LaF_3 nanoparticles.

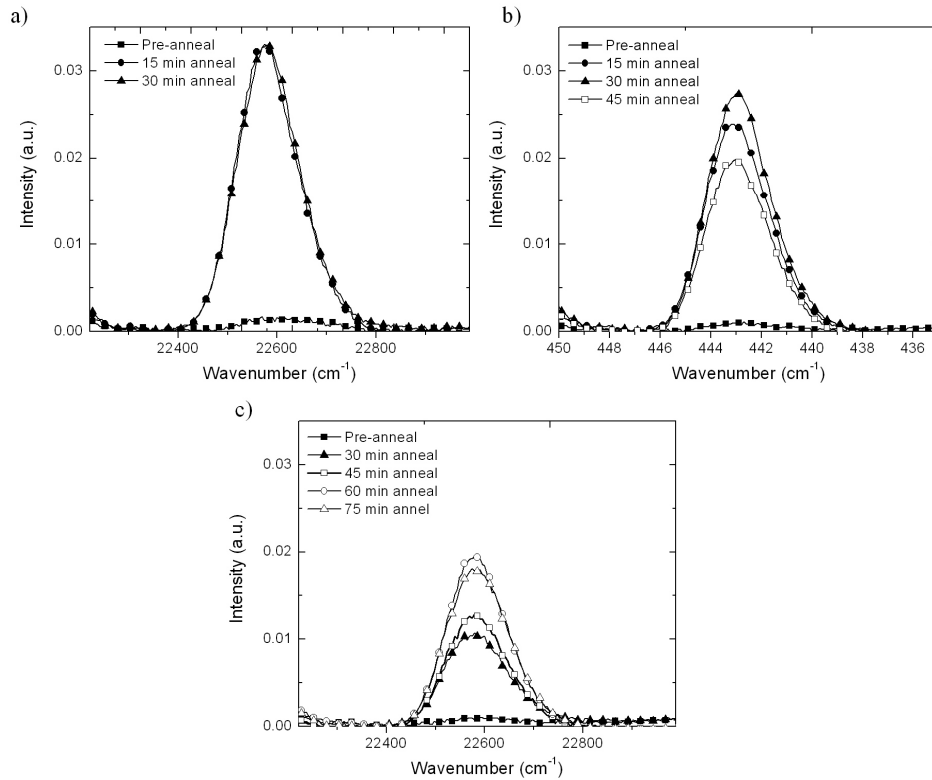


Fig. 4. Phonon sideband spectroscopy of $\text{Eu}_2\text{La}_{0.8}\text{F}_3$ nanoparticles with (a) no intermediate shell and calculated intermediate shell thicknesses of (b) 0.8 nm and (c) 1.3 nm before and after heat-treatment.

is found where the intensity of the PSB peak no longer increases. In Fig. 4(a), it is apparent that within the first 15 minutes the PSB has reached its maximum for a particle with no shell. A particle with a 0.8 nm shell requires 30 minutes to maximize the PSB, Figure 4(b), and a 1.3 nm shell requires 60 minutes. It is also worth to noting that the maximum intensity of the phonon sideband decreases for a particle as the shell thickness increase as seen from Fig. 4(a) to 4c. This is believed to be due to a lower average concentration of Eu^{3+} ions at the surface.

To demonstrate the severity that diffusion can play on the optical properties of a nanoparticle, one can design particles that change colors as a function of their thermal history. Using the same procedure as above core-shell nanoparticles were synthesized with ~ 4.3 nm diameter core and a ~ 5 nm thick shell. The core was doped with 3% Eu^{3+} and the shell was undoped LaF_3 .

The emission spectra of these particles before and after heat-treatment are shown in Fig. 5. Before heat-treating it can be seen that there is no emission from the $^5\text{D}_3$ and $^5\text{D}_2$ energy levels. The same particles were then heated to 750°C for 1 hour. The emission spectrum was then measured under identical conditions as shown by the solid line in Figure 5. The increase in the emissions from the $^5\text{D}_3$ and $^5\text{D}_2$ energy levels are attributed to the Eu^{3+} ions of the core diffusing into the shell. As this occurs, the average ion-ion distances increase and the effective loading level of the particles approaches 0.3 mol%. At such doping levels, the quenching of the Eu^{3+} is significantly decreased and the $^5\text{D}_3$ and $^5\text{D}_2$ energy levels show strong emissions in the blue and green. It is interesting to note that this generates a white light spectrum with CIE coordinates of $x = 0.342$, $y = 0.330$ which could be of interest as a phosphor. Similar results were also recently noted by Lin, et al.¹³

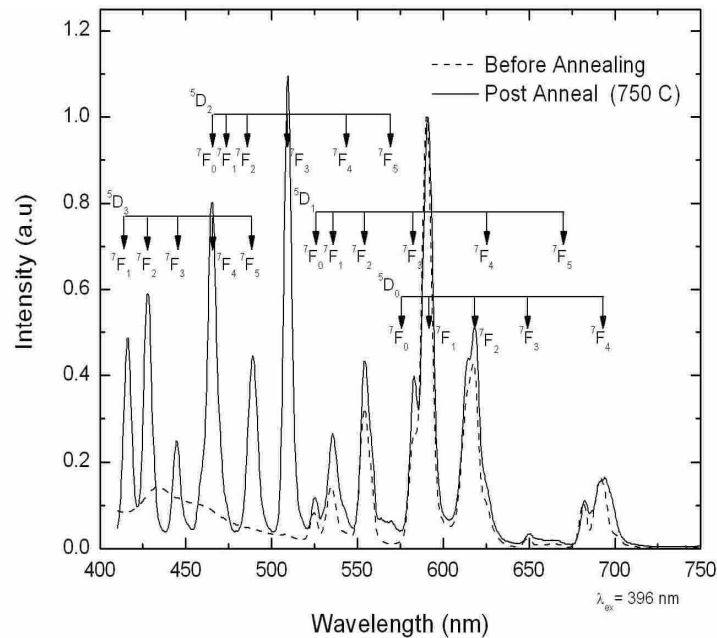


Fig. 5. Emission spectra of core shell particle with 3% Eu^{3+} core before and after annealing.

Lanthanide doped LaF_3 further lends itself to diffusion studies due to the rare-earths affinity to substitutionally dope for the La, making it chemically similar to the radio-isotopic tracers done more conventionally in diffusion studies. Using the spectroscopic and electron microscopic results, an estimation of the diffusion coefficients of lanthanides (specifically here Eu^{3+}) in LaF_3 can be estimated. It is worth noting that some stress inevitably will be present in these core/shell structures due to differences in the lattice parameters between the

regions of differing composition. Such compositional gradients lead to differences in chemical potential, thereby further driving the diffusion process.

The diffusion coefficient was calculated by applying a simple one dimensional approximation¹⁴ using length values equivalent to radii values of 0.75 to 4 nm derived from TEM particle size analysis and assuming steady state diffusion is reached when the spectroscopic properties no longer changes with processing time. For this Eu:LaF₃ system, the average diffusion coefficient was computed to be about 4×10^{-22} m²/s. While this value presumes linear diffusion of the Eu³⁺ from the center of the core to the outermost edge of the LaF₃ shell, it corroborates in order of magnitude with published values for similar materials.¹⁵

It is important to note that this diffusion in core-shell nanoparticles makes their use at elevated temperatures (~ 700 °C) unlikely unless some internal structuring is developed to prevent diffusion. Such higher temperature processing results in diffusion of the dopants and a change in the effective doping level as the rare earth ions are diluted into the shell. In addition, as the authors of Ref. 16 note, solid state reactions can also occur due to particle-host interactions.

4. Summary and conclusions

In conclusion, core-shell nanoparticles have been synthesized and emission and phonon sideband spectroscopy implies the diffusion of Eu³⁺ ions from the core into the shell of the nanoparticles. It was found that at elevated temperatures, the diffusion of the ions is significant enough to result in drastic color changes as emissions from higher energy manifolds are no longer concentration quenched. While this suggests that core-shell particles may not be suitable for high temperature applications, the diffusion rate which is on the same order of magnitude as the bulk rate would suggest that the particles are stable for applications in ambient conditions. It is also possible that steps can be taken to reduce the rate of diffusion in the particles which should be an area of future work.